



Ruthenium silicate (RS-1) zeolite: novel heterogeneous efficient catalyst for synthesis of 2-arylbenzothiazole derivatives

Sachin P. Gadekar¹ · Machhindra K. Lande¹

Received: 10 August 2020 / Accepted: 3 December 2020 / Published online: 4 January 2021
© Springer Nature B.V. 2021

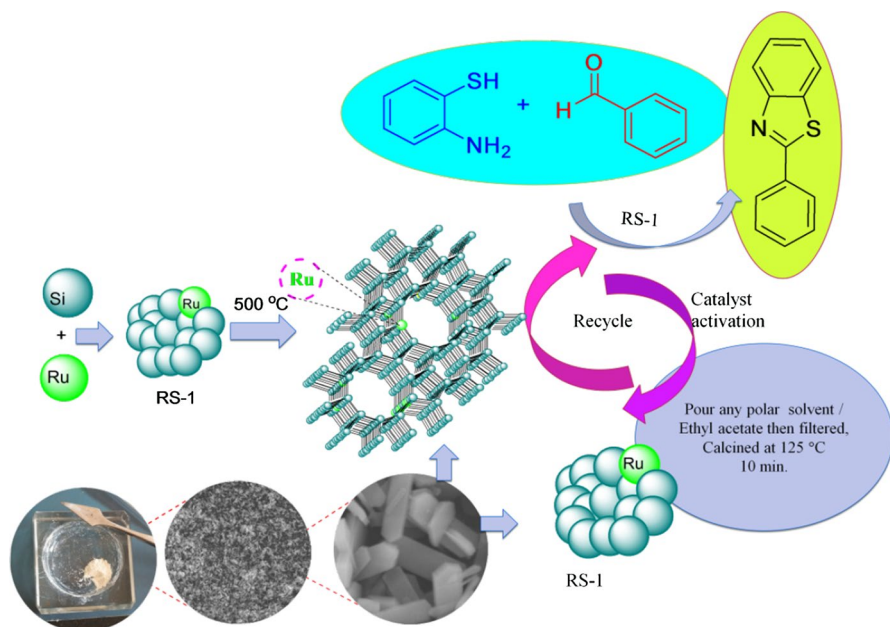
Abstract

Mesoporous silicate and transition metal (Ru^{+3}) containing mesoporous silicate materials or ruthenium silicate $\text{Ru}^{+3}/\text{Si}^{+4}$ where synthesis by using hydrothermal process. Mesoporous ruthenium silicate (RS-1) and zeolite catalyst have been successfully synthesized with variable molar ratio such as (a) Ru:Si 1:100, (b) Ru:Si 1:150, (c) Ru:Si 1:200. The elemental composition, structural morphology, crystal phase and properties and various parameters of the catalyst were examined by Fourier transform infrared spectroscopy, scanning electron microscopy, powder X-ray diffraction. Energy dispersive X-ray pattern/spectroscopy analysis EDX/EDS, where as the activity of obtained catalysts was tested in the Willgerodt–Kindler synthesis between 2-aminothiophenol and substituted aryl aldehyde (1:1 mol) to form a 2-arylbenzothiazole. The novelty of the presented work was the ruthenium (Ru^{+3}) metal impregnations in silicate framework for the synthesis of novel ruthenium silicate (RS-1) zeolite as a catalyst and the investigation of the various parameters, role, its stability and catalytic activity in the Willgerodt–Kindler (combined both Knoevenagel and Maichel addition reaction) synthesis. The developed protocol has several benefits such as short reaction time, mild reaction condition, and good reusability of catalyst.

✉ Machhindra K. Lande
mkl_chem@yahoo.com

¹ Department of Chemistry, Dr. Babasaheb Ambedkar Marathwada University, Aurangabad, Maharashtra 431004, India

Graphic abstract



Keywords Ruthenium silicate (RS-1) · Zeolite catalyst · Willgerodt–kindler · Benzothiazole · Synthesis · Metal insertion

Introduction

Zeolite materials are used as a versatile catalyst in various organic transformations over metal oxide catalyst [1, 2]. The incorporation of metal ion into silicate framework has been reviewed in recent reports; it gives ZSM-5-type structural morphology and MFI topology [1–5]. Transition metal-containing zeolite catalyst material shows good catalytic activity over a long range of temperatures and is more resistant to thermal paths. After completion of reaction, it remains as is, without loss of its catalytic activity, so we call them reusable catalysts. The transition metal ruthenium Ru(III) shows good catalytic activities in various catalytic processes, such as metal hydride transfer reaction, i.e., hydrogenation reactions [6, 7] provide a widely used alternative to direct hydrogenation reactions [8, 9], used as coupling agents, presence of alcohols for alkylation [10–13], as well as oxidation–reduction reaction [14, 15]. Ruthenium metal-containing catalysts are also used in cross-aldol condensation reaction in hormone steroid diastereoselective, direct aldol reactions [16, 17], syntheses of enantiomeric pure pyrrolidine derivatives under very mild conditions and Lewis acid-assisted ring-closing olefin metathesis (RCM) reaction [18]. In C–H activation [19], stereo-pure functionalized asymmetric transfer hydrogenation [20], ruthenium

metal (Ru) containing catalyst use in many more number of organic transformation reaction [21]. Here, we are reporting first time to prepare ruthenium silicate (RS-1) catalyst and used as catalyst for the synthesis of 2-arylbenzothiazole derivative.

Benzothiazole, it consists of five member thiazole-fused ring with benzene ring or substituted aryl benzene. In the 1950s, 2-aminobenzothiazoles first synthesized and was intensively studied as central muscle relaxants; antitumor, anticancer agents, benzoxazole and benzothiazoles are fluorescent used in DNA intercalators for studying Alzheimer $A\beta_{1-42}$ and prion amyloid peptides, also used in dyes such as thioflavin. Benzothiazole, in its presence of unique active methyne center, to give a thermally stable compound, in general two and six positions are more active and shows chemotherapeutic activities [22–27] Fig. 1.

Recently, a researcher has much interest in the synthesis and development of heterocyclic compound containing such as 1, 3-thiazole/oxazole molecular functionality. In the heterocyclic/polycyclic compound containing nitrogen, sulfur and oxygen atom (S, N, and O atom), grant as a unique and versatile scaffold for experimental drug design. They are showing varies activities and have attractive chemical properties, diverse biological, pharmaceutical applications [28] such as antimicrobial [29], antidiabetic, anticonvulsant, anti-inflammatory, antihypertensive, antitubercular DprE1 inhibitors, antioxidant, antimicrobial and cytotoxic activities, imaging agents for Ca^{2+} channel antagonist [30–38] and used as an dopants in light emitting organic electro-luminescent devices [39]. Similarly, also exhibit luminescent and fluorescent properties and therefore they use in designing sensor molecules of specific interest [40, 41]. A lot of methods have been reported for synthesis of benzothiazoles, including some of them are ceric ammonium nitrate (CAN), $Sc(OTf)_3$, H_2O_2 /ceric ammonium, H_2O_2/HCl , bakers' yeast, I_2 , $HClO_4$ /polyaniline [42–45] and some are silica containing catalyst also use, Pd catalyst through C-H activation, lithium bromide (LiBr), $Cu(OAc)_2/MCM-41$, silica gel, montmorillonite K-10, $Cu_{3/2}PMo_{12}O_{40}/SiO_2$ [46–51]. These methods are quite efficient, however most of the catalysts are corrosive, toxic, difficult to separation, and some reaction provide low yields and require long reaction times or use of hazardous and volatile organic solvents ($CHCl_3$, CH_3CN , benzene, toluene), and catalyst is not reusable. To the overcome mentioned above limitation, we have developed new sustainable cost-effective methods. Here, we are firstly reported, new solid acid catalyst ruthenium silicate (RS-1) and used in synthesis benzothiazoles synthesis.

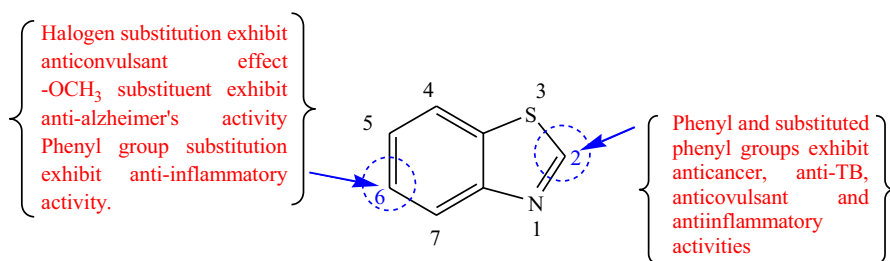


Fig. 1 Benzothiazole consists of active sites of 2 and 6 position methyne center

Experimental

Synthesis of series on ruthenium silicate (RS-1) by hydrothermal method

Ruthenium silicate (RS-1) zeolite was prepared by hydrothermal method from using universal solvent, ruthenium trichloride (RuCl_3) and tetraethyl orthosilicate (TEOS). A solution of tetraethyl orthosilicate (20.83 mL) and tetrapropyl ammoniumhydroxide (TPA-OH) (20 mL, 20%) was added drop wise with vigorous stirring, resulting mixture was stirred for 10 min at room temperature to obtain silica sol. Ruthenium trichloride (RuCl_3) (0.2614 gm) was mixed with 30 mL of dry isopropyl alcohol and stirred vigorously for 10 min, resulting mixture was added drop wise in silica sol with constant stirring at 70–75 °C for 120 min. The pH was maintained alkaline by adding TPAOH and deionized water as a solvent. The viscous gel was formed that was transferred in Teflon-lined stainless steel autoclave treated hydrothermally under a static condition for 24 h. A solid product was filtered and dried in an oven at 100 °C for 1 h. Finally, dried product was calcined in muffle furnace at 500 °C for 4 h under air atmosphere. The resulting material was naturally cooled, characterized and named as RS-1 zeolite. Similarly, a series of RS-1 catalyst was prepared by above same procedure with different lording Ru/Si molar ratio it shows in Table 1.

General procedure for synthesis of 2-arylbenzothiazoles

To the synthesis of 2-arylbenzothiazoles 3 (a-i) from a mixture of 2-aminothiophenol (0.001 mol), benzaldehydes (0.001 mol) and catalytic amount of (0.04 gm) RS-1 under solvent free conditions was refluxed at 90 °C for the prescribed time. The reaction progress was monitored by TLC (ethyl acetate: PET ether = 3:7 as eluent), after completion of the reaction, the product and catalyst were separated by simple filtration, and catalyst was easily separated from the reaction mixture. Finally, crude product obtained was crystallized from ethanol to afford desired pure product. The representative compound was characterized by FTIR ^1H , ^{13}C NMR and HRMS.

Table 1 Synthesis of series of ruthenium silicate (RS-1) by hydrothermal method

Entry	Composition	Ru/Si molar ratio
1	(Ru: Si)	0:1
2	(Ru: Si)	1:100
3	(Ru: Si)	1:150
4	(Ru: Si)	1:200

Results and discussion

X-ray diffraction study

The powder X-ray diffraction pattern of pure SiO_2 and series of RS-1 catalysts calcined at 500°C for 5 h in the presence of air are shown in Fig. 2, respectively. The X-ray diffraction patterns of the pure SiO_2 sample as compare with RS-1 consists of broad diffraction pattern because it is amorphous in nature. The Ru/Si ratio 1: 100 of RS-1 sample exhibit highly intense and sharp peak due to it is crystalline in nature. As per results from powder XRD, only pure silicate and ruthenium metal silicate (RS-1) samples differ very much indicating incorporation of Ru(III) in SiO_2 to form $\text{RuO}_2\text{-SiO}_2$ metal containing ruthenium silicate (RS-1). The study of XRD patterns shows, an interesting observation that the pure SiO_2 sample amorphous structure of SiO_2 shown in Fig. 2a exhibits diffraction pattern of Fig. 2b due to the formation of uniform hexagonal long rods shapes of $\text{RuO}_2\text{-SiO}_2$ framework, the broad peaks were obtained at $2\theta=21.74^\circ$ corresponding to the planes (100) indicates the amorphous structure of SiO_2 shown in Fig. 2a In the XRD pattern of series, RS-1 shows highly intense peaks at $2\theta=8.134^\circ$, 23.286° , 24.138° , 24.776° and corresponding to the planes (101), (332), (033), (313), etc., shown in Fig. 2b. It indicates the orthorhombic structure of RS-1. XRD pattern matches with stimulation data with calcined ZSM-5 structure and MFI topology of synthesized RS-1 zeolite [52–56]. While on the other

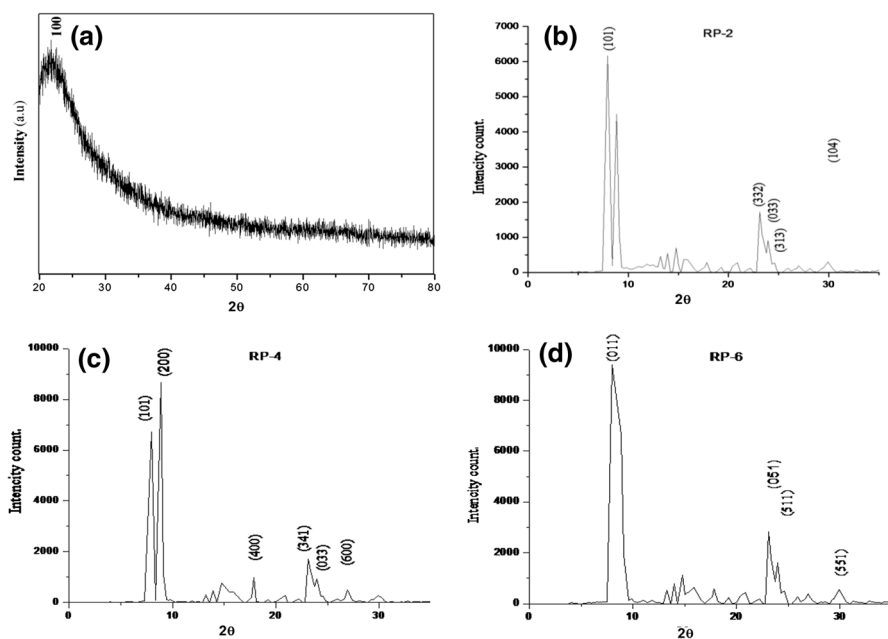


Fig. 2 XRD pattern of **a** pure SiO_2 , **b** RS-1 (Ru/Si 1:100), **c** RS-1 (Ru/Si 1:150), **d** RS-1 (Ru/Si 1:200) calcined at 500°C

hand, Ru/Si increasing ratio of ruthenium (Ru) metal in synthesis of RS-1 zeolite similar spectrum observed. It would be conclude that the RS-1 successfully synthesis with various ratio shown in Fig. 3.

FT-IR analysis

Fig. 4a shows the FT-IR spectrum of the synthesized pure SiO_2 material. The absorption band at 3400 cm^{-1} is due to the Si–OH stretching vibration, 2337 cm^{-1} for glass SiO_2 , 1527 cm^{-1} for the Si–OH bending mode, 1095 cm^{-1} for Si–O stretching vibration and 802 cm^{-1} due to the Si–O–Si bending vibration mode [52–56]. Figure 4b, c show the FT-IR spectrum of RS-1, Ru/Si 1:100 before and after calcined at $500\text{ }^\circ\text{C}$. Materials having absorption band at 3430 cm^{-1} which is due to the Ru–OH/Si–OH stretching vibration. Having absorption band at 3455 cm^{-1} may be due to the stretching vibration of Si–OH–Si or Si–OH–Ru the strong absorption band at $544/548\text{ cm}^{-1}$ is due to the anti-symmetric Ru–O–Ru/Ru–O–Si vibrational mode of RS-1. $1656/1636\text{ cm}^{-1}$ due to the Si–OH bending mode, the broad band at $900\text{ to }1076\text{ cm}^{-1}$ is due to stretching vibration of Ru–O–Si band and 1101 cm^{-1} for Si–O stretching vibration at 795 cm^{-1} due to the Si–O–Si bending vibrational mode [57–63]. In all MFI cases, showing separate IR absorbance bands near 1076 cm^{-1} (internal asymmetric stretch), 795 cm^{-1} (external symmetric stretch) and similarly, 544 cm^{-1} (double ring vibration) and 441 cm^{-1} (T–O bending vibration), if the absorption bands near at 550 cm^{-1} have been assigned to the presence of double 5-membered rings (D5R) [64]. In this synthesis increase Ru/Si ratio 1:150, 1:200, it gives similar spectrum of above RS-1 Ru/Si 1:100 no more difference is observed, then we have concluded the transition metal Ru(III) successfully introduce in the silicate framework and confirm a formation of RS-1 Zeolite with MFI topology.

From the above FTIR, data of Ru^{3+} metal ion inserted in silicate to form and confirm structure of RS-1 (a) Ru:Si 1:100 (b) Ru:Si 1:150 (c) Ru:Si 1:200 used to predict the plausible structure by referencing their IR frequency shown in Fig. 5.

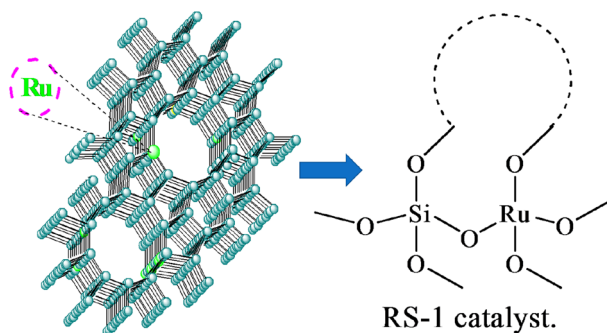


Fig. 3 Reaction, structure and framework of RS-1 zeolite

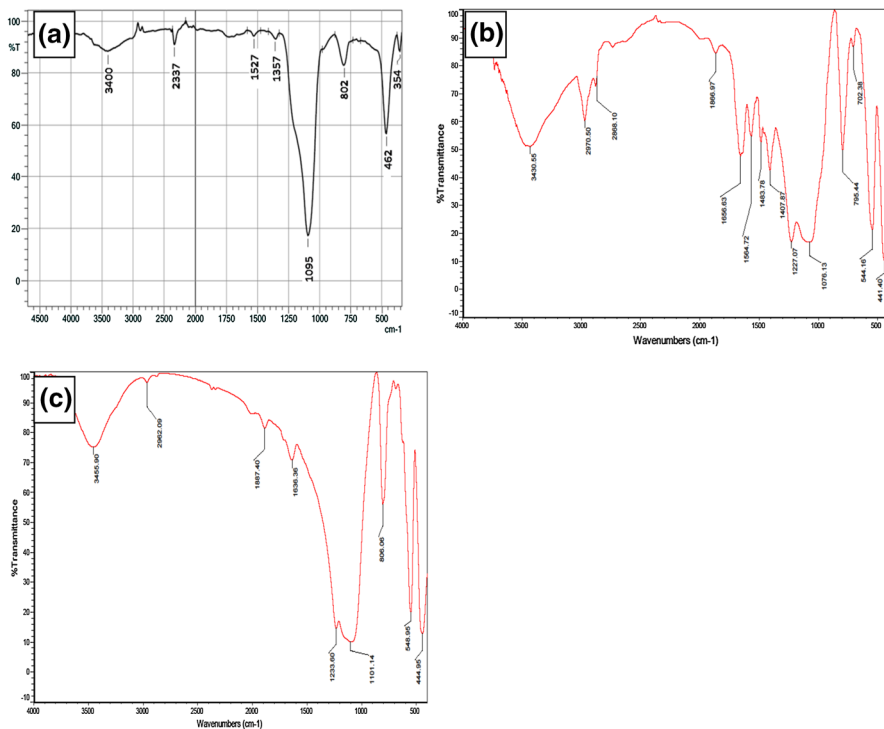


Fig. 4 FTIR spectrum of **a** pure SiO₂ **b** RS-1 Ru/Si 1:100 non-calcined and **c** calcined at 500 °C

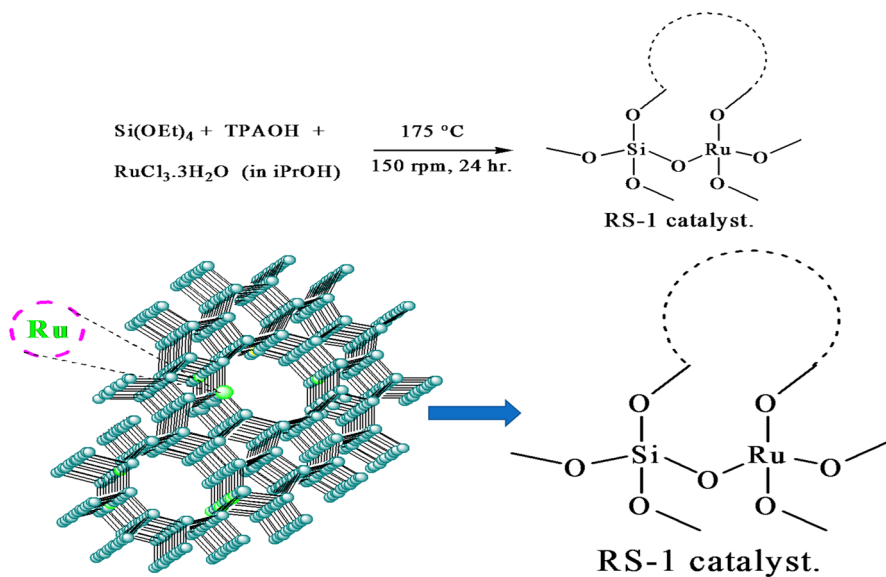


Fig. 5 Plausible structure and framework of RS-1 zeolite

SEM–EDS analysis

The SEM produces artificial 3-dimensional point by point reconstruction of the sample from a signal emitted when the electron beam interacts with the specimen. When the electron beam interacts with the sample, several types of signals are produced. The basic two signals are electron and electromagnetic radiation. If SEM is operated to produce an image using back scattered electrons, it should be noted that resolution is considerably reduced in back scattered mode of operation, because back scattered electrons are generated in a large volume of sample (1–3 nm deep). In this study, it is necessary to consider not only intrinsic instrument resolution, but also interaction of the incident electron beam and the sample. SEM and EDS measurements were carried out to investigate the detailed morphology, surface roughness and structure of the nanoparticles along with element detection.

Figure 6a shows the flakes like structure of SiO_2 , and Fig. 6b indicates the surface morphology of RS-1 shows uniform hexagonal long rods shapes and clearly indicates introduce transition Ru(III) in SiO_2 Silicate material and formation of orthorhombic RS-1 as zeolite catalyst. Figure 6c and d show same structure of similar synthesis or RS-1 increasing ratio. No more structural changes of framework change in increasing loading Ru/Si ratio [65, 66]. (Scheme 1).

SEM and EDS measurements were carried out to investigate the detailed morphology, in order to study the surface morphology and structural properties of

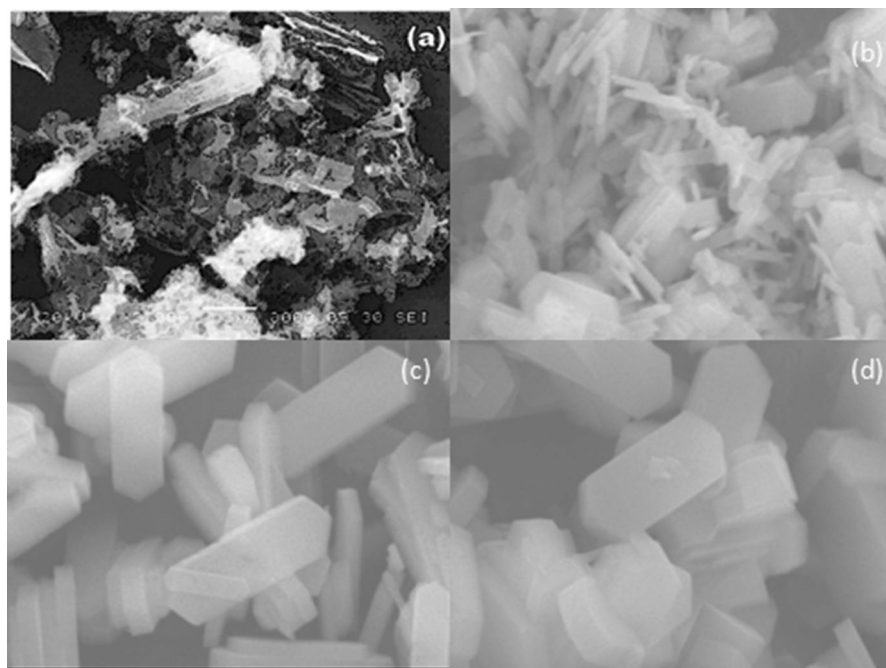
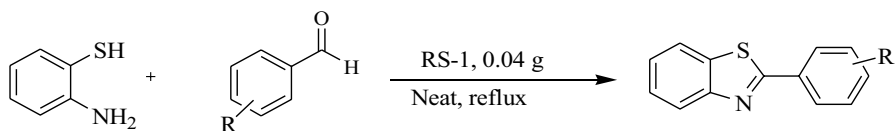


Fig. 6 SEM image of **a** SiO_2 , **b** RS-1 Ru/Si 1:100, **c** RS-1 Ru/Si 1:150, **d** RS-1 Ru/Si 1:200 calcined at 500 °C



Scheme 1 Synthesis of RS-1 zeolite catalyst and catalytic activity tested in synthesis of Aryl 2-arylbenzothiazole

synthesized catalyst RS-1 materials along with elements detection. SEM images show uniform hexagonal long rods shapes and orthorhombic crystals, which is characteristic morphology of RS-1 type zeolites. The elemental composition of RS-1 is shown in Fig. 7 which confirm the presence Ru, Si and O, (atom %), respectively (Table 2), and Ru, Si and O peaks can be obviously found in the spectrum which indicate that the RS-1 zeolite is successfully prepared with corresponding empirical formula $\text{Ru}_1 \text{Si}_{181} \text{O}_{459}$.

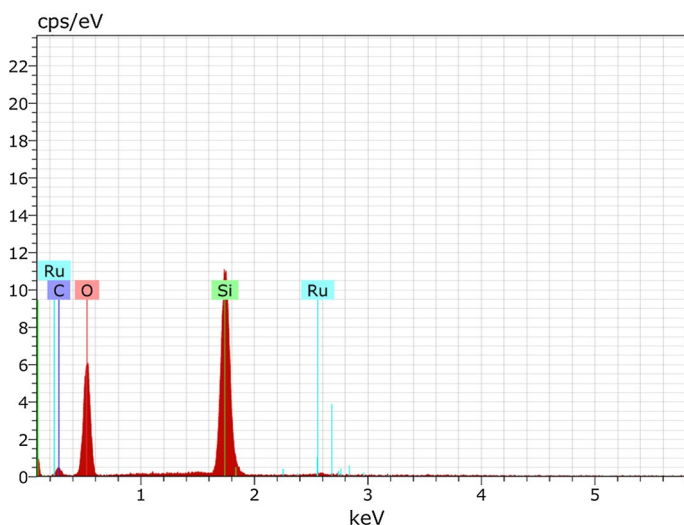


Fig. 7 EDS spectrum of RS-1 (1:100) calcined at 500 °C

Table 2 EDS mass and atom of RS-1(1:100) calcined at 500 °C

Element	Mass (%)	Atom (%)
O	52.11	59.61
Si	36.25	23.52
C	10.92	16.64
Ru	0.71	0.13
Total	100.00	100.00

Table 3 Solvent optimization of model reaction (3a)

Entry	Solvent	Time (min)	Yield (%) ^a
1	Solvent free	200	Trace
2	CH ₂ Cl ₂	200	40
3	H ₂ O	200	50
4	MeCN	200	70
5	DMF	200	70
6	EtOH	100	80
7	Solvent free	30	93

^aIsolated yields**Table 4** Synthesis of (3a) using different catalysts

Entry	Catalyst	Time (min)	Yield (%) ^a
1	Ammonium chloride 70 mol % in Et-OH	30	70 [65, 66]
2	TiCl ₄ /Sm, THF 40 °C,	10	70 [67]
3	FeCl ₃ 10%	60	65 [47, 48]
4	RS-1, 0.04 g Solvent free	30	93 our result

^aIsolated yields

Catalytic activity results

Synthesized solid acid catalyst ruthenium silicate (RS-1) (Ru/Si, 1:100) zeolite used in synthesis of aryl benzothiazole by using 2-aminothiophenol (1 mmol) and substituted aryl aldehyde (1 mmol), in the presence of RS-1 catalyst (0.04 g) reflux at 90 °C under solvent free condition in model reaction (3a) and optimize the reaction conditions. We are evaluated the effect of dissimilar solvents such as CH₂Cl₂, EtOH, H₂O, MeCN, DMF and solvent free condition on the reaction rate under the same reaction conditions, solvent free reaction afforded the products in higher yield and shorter reaction time (Table 3). Amount of catalyst also optimized, the 0.04 g catalyst gives 93% the highest yield. In this study, the effect of different catalysts is investigated and shown in (Table 4), but in titanium chloride and FeCl₃ catalyst was employed, the corresponding product yield was obtained 70% and 65%, respectively (Table 4, entry 2 and 3). However, when RS-1 zeolite catalyst was employed, the corresponding product gives the highest yield 93% (model reaction 3a). We have found that RS-1 as a better catalyst with respective to reaction time and good yield of obtained products.

In next steps, we have investigated the amounts of RS-1 catalyst (10, 20, 30, 40, 50, mg). The optimum yield of the substituted aryl benzothiazole was obtained, when 0.04 gm of RS-1 zeolite catalyst was used Table 5. Therefore, in an optimized reaction condition, 2-aminothiophenol (0.001 mol), aryl benzaldehydes (0.001 mol),

Table 5 Optimization of RS-1 catalyst amount for model reaction (3a)

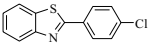
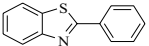
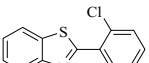
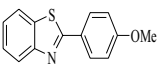
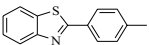
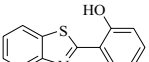
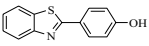
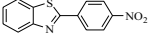
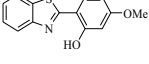
Entry	Catalyst (mg)	Yield (%) ^a
1	10	20
2	20	40
3	30	80
4	40	93
5	50	93

^aIsolated yields

wt. of RS-1 catalyst (0.04 g, Ru/Si, 1:100), refluxed in solvent free for completion of reaction time (10–13 min) product/ derivatives are shown in Table 6.

In general study of this over all process, several examples illustrating this method, in the synthesis of those polyfunctionalized aryl benzothiazole were studied, and results are summarized in Table 6. The effect of different substituent's on the aromatic aldehyde ring did show expected strong effects in terms

Table 6 Synthesis of aryl benzothiazole derivatives using RS-1 catalyst

Entry	Product structure	R ₁	Yield (%) ^a	M.P (°C)	
				Found	Lit [23, 39]
3a		4-Cl	93(92,92,91.8) ^b	115–116	114–116
3b		H	93	114–115	111–113
3c		2-Cl	91	82–84	81–82
3d		4-OMe	91	122–124	119–121
3e		4-Me	92	88–89	86–89
3f		2-OH	90	130–132	131–132
3g		4-OH	91	227–229	230–234
3h		4-NO ₂	93	329–230	230–131
3i		2-OH 4-ome	85	130–132	–

Reaction Condition 2-aminothiophenol (0.001 mol), aryl benzaldehydes (0.001 mol), wt of RS-1 catalyst (0.04 gm, Ru/Si 1:100), refluxed in solvent free;

^aYield after consecutive cycles, ^bIsolated yields.

of yields as well as completion of reaction time under these reaction conditions. Substituted aryl aldehyde containing electron-withdrawing groups (NO_2 and Cl) or electron-donating groups (OMe , OH groups) was employed and they were found to react well to give the corresponding aryl benzothiazoles derivatives in good to excellent yields. Aromatic aldehydes having electron-withdrawing groups on the aromatic ring (Table 6, entries 3a, h) react faster than electron-donating groups (Table 6, entry 3d, g). Schematic plausible reaction mechanism of aryl benzothiazole derivatives is shown in Fig. 8

We also examined the recycling performance of RS-1 catalyst and investigated by using a 3a model reaction. After the catalyst separation, before use catalyst needs to the activation, the catalyst was washed with polar solvent for two to three times and dried at $120\text{ }^\circ\text{C}$ for 10 min and then used directly with fresh substrates under identical conditions with no further purification. It was shown that, the catalyst could be used for three times runs without loss of the product yield as well as its catalytic performance shown in Fig. 9. The catalyst having easy recycling performance is also an attractive property for the ecological protection and financial reasons.

Spectral data of representative compound:

2-(benzo[d]thiazol-2-yl)-5-methoxyphenol (3i); ^1H NMR (400 MHz, CDCl_3) δ (ppm):12.7 (S,1H, Ar-OH), 8–6.8(m, 7H, Ar-H), 3.9 (t, 3H, CH_3) IR (KBr):

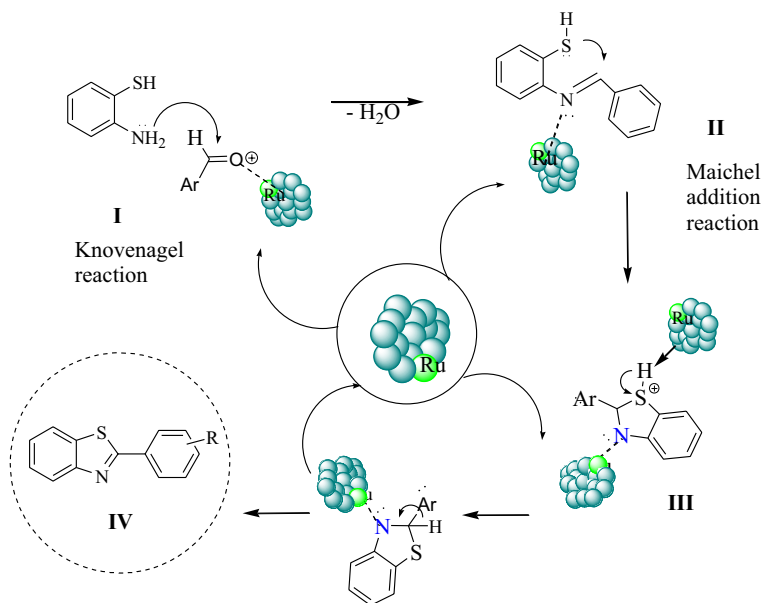


Fig. 8 Schematic plausible reaction mechanism of aryl benzothiazole derivatives

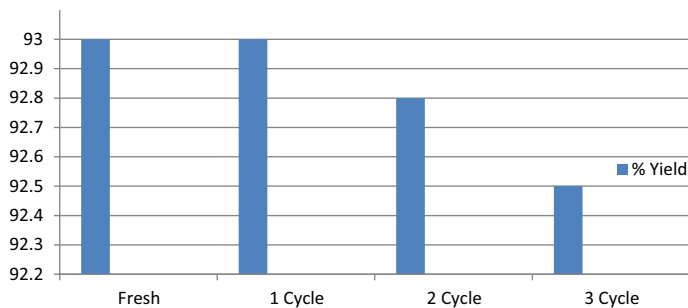


Fig. 9 Reusability test of RS-1 for the synthesis of 3i

2970, 2991, 2678, 1672, 1594, 1508, 1328, 1234, 1091., 986, 707; ^{13}C NMR (50 MHz, CDCl_3) δ (ppm): 169, 151, 159, 148, 132, 126, 125, 122, 121, 120, 119, 116, 114, 56, HR-MS: m/z 258.0467.181 (M^+).

Conclusion

In summary, during the synthesis, crystal growth and grain size of resulting zeolite RS-1 catalyst, estimated ratio significantly not affected with same time period. Where found no more effected on crystal growth and uniform look like long rods shape but XRD, SEM and EDX analysis technique helps to actual structure analysis. Synthesized ruthenium silicate (RS-1) has given as uniform hexagonal long rods shapes, highly crystalline morphology with similar structural morphology is as ZSM-5-type and MFI topology. Hence, we have successfully synthesis, a strong heterogeneous, Lewis acid, solid acid RS-1 catalyst and applied in Lewis acid catalyzed reactions. On the other hand, we have developed a new straight forward and efficient methodology for the preparation of 2-arylbenzothiazole and its derivatives via ruthenium silicate (RS-1) catalyst in solvent free condition. The RS-1 catalyst is high thermal stability and reusability without any noticeable loss of reactivity. The mild reaction conditions and simplicity of the procedure offers several advantages such as shorter reaction time, simple experimental procedure, high yield and catalyst can be recycled and reused.

Acknowledgments We are grateful to the Head, Department of Chemistry, Dr. B.A.M. University, Aurangabad-431004 (MS), India for providing the laboratory facility, and to the STIC Cochin and SAIF Chandigarh characterization facilities.

Funding The corresponding author MKL is thankful to UGC New Delhi for providing grant under major research project F. No. 43-184/2014 (SR).

References

1. T. Jaimol, A.K. Pandey, A.P. Singh, *J Mol Catal A: Chem* **170**, 117 (2001)
2. M. Breyse, M. Cattenot, V. Kougonas, J.C. Lavalley, F. Mauge, J.L. Portefaix, J.L. Zotin, *J Catal* **168**(2), 143 (1997)
3. S.K. Das, P.K. Dutta, *Micropor Mesopor Mater* **22**(1–3), 475 (1998)
4. P.K. Dutta, *J Incl Phenom Mol Recogit Chem* **21**(1–4), 215 (1995)
5. J.Q. Zhong, J. Kestell, I. Waluyo, S. Wilkins, C. Mazzoli, A. Barbour, K. Kaznatcheev, M. Shete, M. Tsapatsis, J.A. Boscoboinik, *J Phys Chem C* **120**, 8240 (2016)
6. T.D. Nixon, M.K. Whittlesey, J.M.J. Williams, *Tetrahedron Lett* **52**, 6652 (2011)
7. V. Sydoruk, S. Levyska, N. Shcherban, S. Khalameida, *Res Chem Intermed* **46**(9), 3997 (2020)
8. J.G. de Vries, C.J. Elsevier, *The Handbook of Homogeneous Hydrogenation* (Wiley-VCH Verlag GmbH and Co KgaA, Weinheim, 2007).
9. S. Burling, M.K. Whittlesey, J.M. Williams, *Adv Synth Catal* **347**, 591 (2005)
10. M.G. Edwards, R.F.R. Jassar, B.M. Paine, D.J. Shermer, M.K. Whittlesey, J.M.J. Williams, D.D. Edney, *Chem Commun* **1**, 90 (2004)
11. P.A. Slatford, M.K. Whittlesey, J.M.J. Williams, *Tetrahedron Lett* **47**, 6787 (2006)
12. S. Burling, B.M. Paine, D. Nama, V.S. Brown, M.F. Mahon, T.J. Prior, P.S. Pregosin, M.K. Whittlesey, J.M. Williams, *J Am Chem Soc* **129**, 1987 (2007)
13. M.H.S.A. Hamid, J.M.J. Williams, *Tetrahedron Lett* **48**, 8263 (2007)
14. E.Y. Lee, Y. Kim, J.S. Lee, J. Park, *Eur J Org Chem* **2009**, 2943 (2009)
15. P. Veerakumar, A. Ramdass, S. Rajagopal, *J Nanosci Nanotechnol* **13**, 4761 (2013)
16. K. Tabatabaeian, M. Mamaghani, N.O. Mahmoodi, E. Keshavarz, *ARKIVOC* **2009**, 68 (2009)
17. K. Tabatabaeian, E. Keshavarz, M. Mamaghani, N. O. Mahmoodi, *Org. Chem. Int.* **5**, 325291 (2011)
18. Q. Yang, W.J. Xiao, Z. Yu, *Org Lett* **7**(5), 871 (2005)
19. D. Wagner, S. Brase, *Beilstein J Org Chem* **11**, 431 (2015)
20. M. Jeran, A.E. Cotman, M. Stephan, B. Mohar, *Org Lett* **19**, 2042 (2017)
21. T. Naota, H. Takaya, S.I. Murahashi, *Chem Rev* **98**, 2599 (1998)
22. A. Rana, N. Siddiqui, S.A. Khan, *Indian J Pharm Sci* **69**(1), 10 (2007)
23. R. Ali, N. Siddiqui, *Hindawi Publ Corp J Chem* **2013**, 1 (2013)
24. S. Stefansson, D.L. Adams, T. Cha-Mei, *BioTechniques* **52**, 1 (2012)
25. K.B. Akhil, A.P. Khyathi, A.R. Parikh, *Indian J Chem* **38B**, 628 (1999)
26. B. Kaya, W. Hussin, L. Yurttas, G. Turan-Zitouni, H.K. Gençer, M. Baysal, A.B. Karaduman, Z.A. Kaplanckl, *Drug Res.* (2017)
27. P.P. Prabhu, T. Panneerselvam, C.S. Shastri, A. Sivakumar, S.S. Pande, *J Saudi Chem Soc* **19**, 181 (2015)
28. S. Banerjee, S. Payra, A. Saha, G. Sereda, *Tetrahedron Lett* **55**, 5515 (2014)
29. T. Al-Harthy, W.M. Zoghaib, R. Stoll, R. Abdel-Jali, *Monatsh Chem* **149**, 645 (2018)
30. Da.-C. Liu, H.-J. Zhang, C.-M. Jin, Z.-S. Quan, *Molecules* **21**, 164 (2016)
31. E. Stone, F. Citossi, R. Singh, B. Kaur, M. Gaskell, P. Farmer, A. Monks, C. Hose, M. Stevens, C. Leong, M. Stocks, B. Kellam, M. Marlow, T. Bradshaw, *Bioorg Med Chem* **23**, 6891 (2015)
32. R. Ali, N. Siddiqui, *Arch Pharm Chem Life Sci* **348**, 254 (2015)
33. R. Chikhale, S. Menghani, R. Babu, R. Bansode, G. Bhargavi, N. Karodia, V. Rajasekharan, A. Paradkar, P. Khedekar, *Eur J Med Chem* **96**, 30 (2015)
34. V. Patil, K. Nandre, S. Ghosh, V. Rao, B. Chopade, B. Sridhar, S. Bhosale, S. Bhosale, *Eur J Med Chem* **59**, 304 (2013)
35. G. Yadav, S. Ganguly, *European J Med Chem* **97**, 419 (2014)
36. P. Deprez, T. Temal, H. Jary, M. Auberval, S. Lively, D. Guedin, J. Vevert, *Bioorg Med Chem Lett* **23**, 2455 (2013)
37. D. Seenaiiah, P. Reddy, G. Reddy, A. Padmaja, V. Padmavathi, N. Krishna, *Eur J Med Chem* **77**, 1 (2014)
38. L. Racane, M. Cindric, N. Perin, P. Roskaric, K. Starcevic, T. Masek, M. Mauric, J. Dogan, G. Karminski-Zamola, *Croat Chem Acta* **90**(2), 187 (2017)
39. H.-Y. Fu, X.-Y. Sun, X.-D. Gao, F. Xiao, B.-X. Shao, *Synth Metals* **159**, 254 (2009)
40. D. Champiat, N. Matas, B. Monfort, H. Fraass, *Luminescence* **16**, 193 (2001)
41. J.C. Day, L.C. Tisi, M.J. Bailey, *Luminescence* **19**, 8 (2004)
42. K. Bahrami, M.M. Khodaei, F. Naali, *J Org Chem* **73**, 6835 (2008)

43. H.Y. Guo, J.C. Li, Y.L. Shang, *Chinese Chem Lett* **20**, 1408 (2009)
44. T. Itoh, K. Nagata, H. Ishikawa, A. Ohsawa, *Heterocycles* **62**, 197 (2004)
45. Y. Li, Y.L. Wang, J.Y. Wang, *Chem Lett* **35**, 460 (2006)
46. C.H. Gill, M.D. Nikam, P.S. Mahajan, A.V. Chate, S.K. Dabhade, P.V. Badadhe, *Res Chem Intermed* **41**, 7509 (2015)
47. M. Kodomari, Y. Tamaru, T. Aoyama, *Synth Commun* **34**, 3029 (2004)
48. A. Banerjee, A. Bera, S. Guin, S.K. Rout, B.K. Patel, *Tetrahedron* **69**, 2175 (2013)
49. U.R. Pratap, J.R. Mali, D.V. Jawale, R.A. Mane, *Tetrahedron Lett* **50**, 1352 (2009)
50. G.F. Chen, H.M. Jia, L.Y. Zhang, B.H. Chen, J.T. Li, *Ultrason. Sonochem* **20**, 627 (2013)
51. R. Fazaali, H. Aliyan, *Appl Catal A* **353**, 74 (2009)
52. R. Nandanwar, P. Singh, F.Z. Haque, *ACS J* **5**(1), 1 (2015)
53. P. Djomgoue, D. Njopwouo, *J Surface Eng Mater Adv Tech* **3**, 275 (2013)
54. F. Adam, S. Balakrishnan, P.L. Wong, *J Phy Sci* **17**(2), 1 (2006)
55. M.M. Treacy, J.B. Higgins, *Collection of Simulated XRD Powder Patterns for Zeolites*, 4th edn. (Elsevier, New York, 2001), p. 238
56. I. Diaz, E. Kokkoli, O. Terasaki, M. Tsapatsis, *Chem Mater* **16**, 5226 (2004)
57. C.A. GeiGer, G.E.R. Rossman, *Am Mineral* **103**, 384 (2018)
58. R. Strobel, A. Baiker, S.E. Pratsinis, *Adv Powder Technol* **17**, 457 (2006)
59. N. Maxim, *Metal silsesquioxanes as precursors to microporous metallosilicates*. Ph.D. Thesis. Eindhoven University of Technology. (2002)
60. W.J. Stark, R. Strobel, D. Gunther, S.E. Pratsinis, A. Baiker, *J Mater Chem* **12**, 3620 (2002)
61. L. Lang, X. Liu, B. Zhang, *Appl Surf Sci* **255**(9), 4886 (2009)
62. R. Szostak, *Molecular Sieve*, 2nd edn. (Blackie-Academic Professional, London, 1998), p. 306
63. P. LOSCH, Ph. D. Thesis, *Synthesis and Characterisation of Zeolites, their Application*. (2016)
64. Online data, 10_chapter 3, Ph. D. Thesis, *Synthesis and Characterization of In and Ru incorporated MFI Zeolite*, page. 1–129
65. A.A. Yelwande, M.E. Navgire, D.T. Tayde, B.R. Arbad, M.K. Lande, S. Afr, *J Chem* **65**, 131 (2012)
66. B. Maleki, H. Salehabadi, *Eur J Chem* **1**, 377 (2010)
67. Da.-Q. Shi, S.-F. Rong, G.L. Dou, *Syn Comm* **40**, 2302 (2010)

Publisher's Note Springer Nature remains neutral with regard to jurisdictional claims in published maps and institutional affiliations.